UNVEILING THE ACTIVE NUCLEUS OF XBONGS

F. Civano[1,2], A. Comastri[1], M. Mignoli[1], C. Vignali[2,1], F. Fiore[3], and F. Cocchia[4]

[*]**on behalf of the HELLAS2XMM Collaboration**

[1]INAF – Osservatorio Astronomico di Bologna, Bologna, Italy
[2]Dipartimento di Astronomia, Università di Bologna, Bologna, Italy
[3]INAF – Osservatorio Astronomico di Roma, Monteporzio-Catone , Italy
[4]INAF – Osservatorio Astronomico di Brera, Milano, Italy

ABSTRACT

We present the results of a detailed morphological analysis of three X–ray Bright Optically Normal Galaxies (XBONGs) detected in the HELLAS2XMM survey and observed with ISAAC@VLT in the J and K_s bands. These sources have relatively high X–ray luminosity and are associated with galaxies showing no obvious signature of AGN activity in their optical spectra. In deep near–infrared observations two out of the three sources reveal a nuclear point–like excess with respect to the galaxy starlight.

Key words: active galaxies; X-rays; surveys.

1. INTRODUCTION

One of the most interesting findings of the recent Chandra and XMM-*Newton* surveys consists in the discovery of luminous ($L_{2-10keV} \simeq 10^{41-43}$ erg s^{-1}) hard X–ray sources hosted by normal galaxies whose optical spectra are relatively featureless (i.e. without any obvious emission lines like $H\alpha$, $H\beta$, $[OIII]$; Barger et al. 2001; Comastri et al. 2002). The X–ray luminosities, the X–ray-to-optical flux ratio[1] ranging between that of truly normal galaxies (X/O$\sim$–2) and that of AGN (X/O$\sim$0) and their hard X–ray spectra, as inferred from the X–ray colors, all suggest that some kind of activity is taking place in their nuclei.

In order to explain the lack of optical emission lines and the multiwavelength properties of XBONGs, different interpretations have been suggested:

- Heavy obscuration by Compton–thick gas covering almost 4π at the nuclear X–ray sources prevents ionizing optical and UV photons from escaping, thus hampering the formation of the Narrow Line Regions (NLRs). Such a possibility is favoured by Comastri et al. (2002) to explain the multiwavelength behaviour of P3, the XBONG prototype.
- In a Radiatively Inefficient Accretion Flow (RIAF) model, a featureless hard X–ray spectrum is expected, with a negligible contribution in the optical and UV bands, which are therefore dominated by the host galaxy stellar light (Yuan & Narayan 2004).
- Diffuse emission, associated with a small group of galaxies or a close pair, unresolved by XMM observations.
- Dilution of nuclear emission from the host galaxy starlight (Georgantopoulos and Georgakakis 2005). Such an effect might be important if the ground-based spectroscopic observations are performed with relatively wide slits (Severgnini et al. 2003), or the sources are at high redshifts (Moran et al. 2002).

Although some of the above mentioned explanations provide a good description of the observed properties of a few objects, the nature of XBONGs is still subject of debate.

In order to search for weak AGN signatures, we have pursued an alternative approach which is based on deep near–infrared (NIR) imaging of relatively bright XBONGs. In the NIR the nuclear emission (either obscured or reddened) should rise over the stellar light. We present the results obtained applying the surface brightness decomposition tecnique to J and K_s good–quality images of a small sample of XBONGs.

2. THE SAMPLE

The sample presented here includes three sources, serendipitously detected in the 2–10 keV band, from the

[1] $X/O = \log \frac{f_X}{f_R} = \log f_X + C + \frac{R}{2.5}$

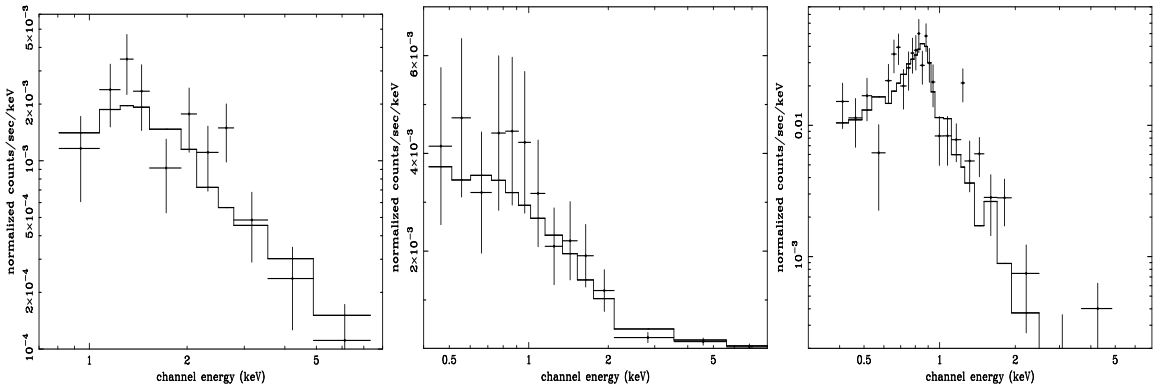

Figure 1. XMM-Newton (pn) spectra of the sources PKS 03120018, PKS 03120017 and Abell 2690013. The X-ray parameters after fitting the spectra with an absorbed power–law model (PKS 03120018 and PKS 03120017) and with a thermal model (Abell 2690013) are reported in Table 1.

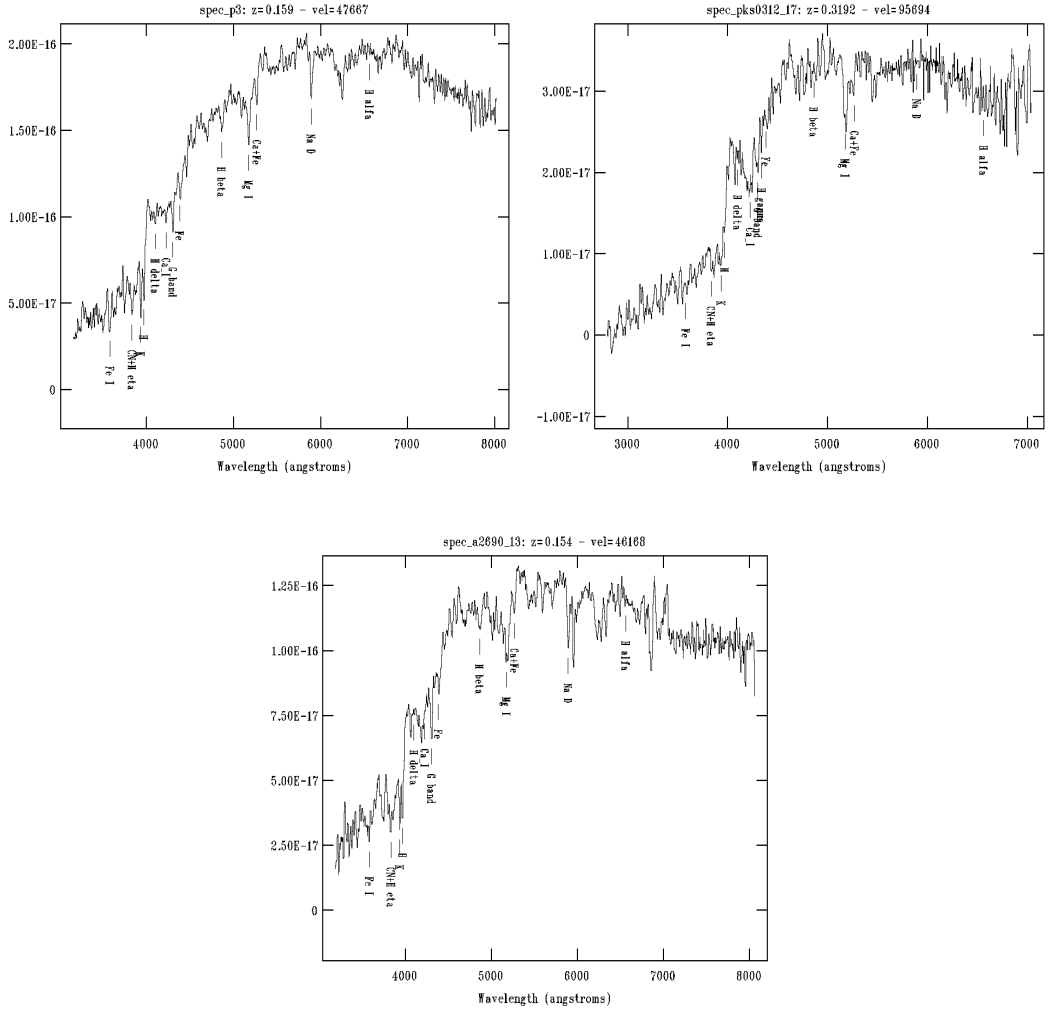

Figure 2. Optical spectra of the sources PKS 03120018, PKS 03120017 (top) and Abell 2690013 (bottom) taken with the ESO 3.6m telescope.

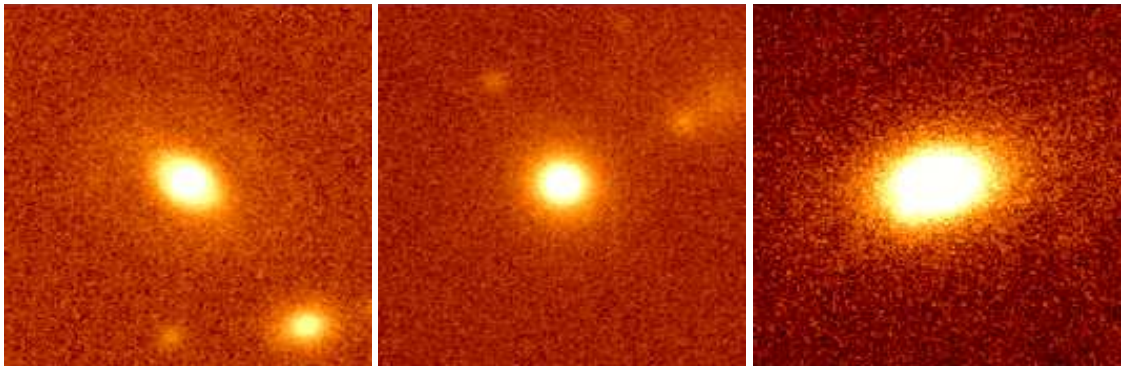

Figure 3. K_s–band images: PKS 03120018, PKS 03120017 and Abell 2690013. The image size is 15"× 15".

Table 1. X–ray spectral analysis parameters.

id	Γ	N_H (cm^{-2})	$\chi^2_{d.o.f}$
PKS 03120017	$2.11^{+0.82}_{-0.36}$	$6.86^{+7.94}_{-4.58}\times 10^{21}$	9.6/9
PKS 03120018	$2.40^{+0.62}_{-0.40}$	$< 2.11\times 10^{21}$	3.7/11
id	kT (keV)	–	$\chi^2_{d.o.f}$
Abell 2690013	0.75± 0.06		42.5/27

HELLAS2XMM 1dF sample: two objects in the PKS 0312 field (03120018 and 03120017) and one in the Abell 2690 field (2690013). The source redshfits are 0.159, 0.319 and 0.154, respectively. Their X–ray and optical properties are discussed in Fiore et al. (2003) and Perola et al. (2004). The X–ray spectral parameters are reported in Table 1 and the spectra are shown in Figure 1; a careful X-ray analysis will be present in Civano et al. (2006). The optical spectra (Figure 2) have been taken with the ESO 3.6m telescope (slit width 1.5"–2"). The upper limits on the typical AGN optical emission line $[OIII]$ in our good signal-to-noise ratio spectra are $F[OIII]_{5007\mathring{A}} < 4\times 10^{-18}$ erg cm^{-2} s^{-1}, one order of magnitude fainter than that expected from the X–ray luminosities for typical AGN emission (see also Cocchia et al. in prep. and references therein).

3. NEAR INFRARED ANALYSIS

The near–infrared observations have been carried out using the VLT (Very Large Telescope) with the Infrared Spectrometer and Array Camera (ISAAC). The ISAAC images were taken in two near–IR bands (the J and K_s filters) and were reduced using the DIMSUM[2] package, following standard procedures. Total exposure times for each galaxy were 600 sec in J and 1800 sec in K_s. The effective seeing on the final frames ranges between 0.5 and 0.8 arcsec (FWHM). The K_s images obtained for the three sources are shown in Figure 3.

[2]Deep Infrared Mosaicing Software, developed by P.Eisenhardt, M.Dickinson, A.Stanford and J.Ward., and available at the site `ftp://iraf.noao.edu/contrib/dimsumV2`

The surface brightness decomposition has been performed with GALFIT (Version 2.0.3b, Peng et al. 2002), a two dimensional algorithm that extracts structural parameters from galaxy images combining several analytical models. The fitting procedure was performed in both the J and K_s bands which allows to cross-check the results and search for a possible color trend. In order to better constrain the galaxy structural parameters, the fit was first performed in the J band, where the AGN contribution is resulted to be lower. Then we fitted the K_s band where the AGN contribution (if present) to the total light is expected to be more important.

For the analysis we proceed as follows. The host galaxy surface brightness was modeled with a de Vaucouleurs profile

$$\mu(r) = \mu_e \, \mathrm{e}^{-7.67\left[(\frac{r}{r_e})^{1/4}-1\right]} \qquad (1)$$

where r_e is the effective radius and μ_e is the surface brightness at the effective radius. If a residual emission in the innermost region is still present after the fitting procedure, we added the contribution of a point-like source. The latter is modeled by the average profile of several stars in the field nearby each source. For both bands we performed the GALFIT analysis without and with the central unresolved component down to the images magnitude limit for point-like sources (J(lim)=22 and K_s(lim)=21.5).

In two out of the three sources the addition of a nuclear unresolved component significantly improves the statistical quality of the fit. The residual images of PKS 03120018 and 03120017 are shown in Fig. 4 and the fitting results are reported in Table 2. There is no evidence of a point-like source in Abell 2690013. This result is consistent with X–ray spectral and spatial analysis: the X–ray spectrum of Abell 2690013 is well represented by a thermal model (see Table 1) and the X–ray contours are suggestive of diffuse emission centered on the optical galaxy (see Fig. 5).

Once the nuclear component is subtracted, the host galaxy parameters (m_{host}, r_e) and the J–K_s colors are in good agreement with the K_s–band luminosity–radius relation (Pahre 1999) and the color for elliptical galaxies

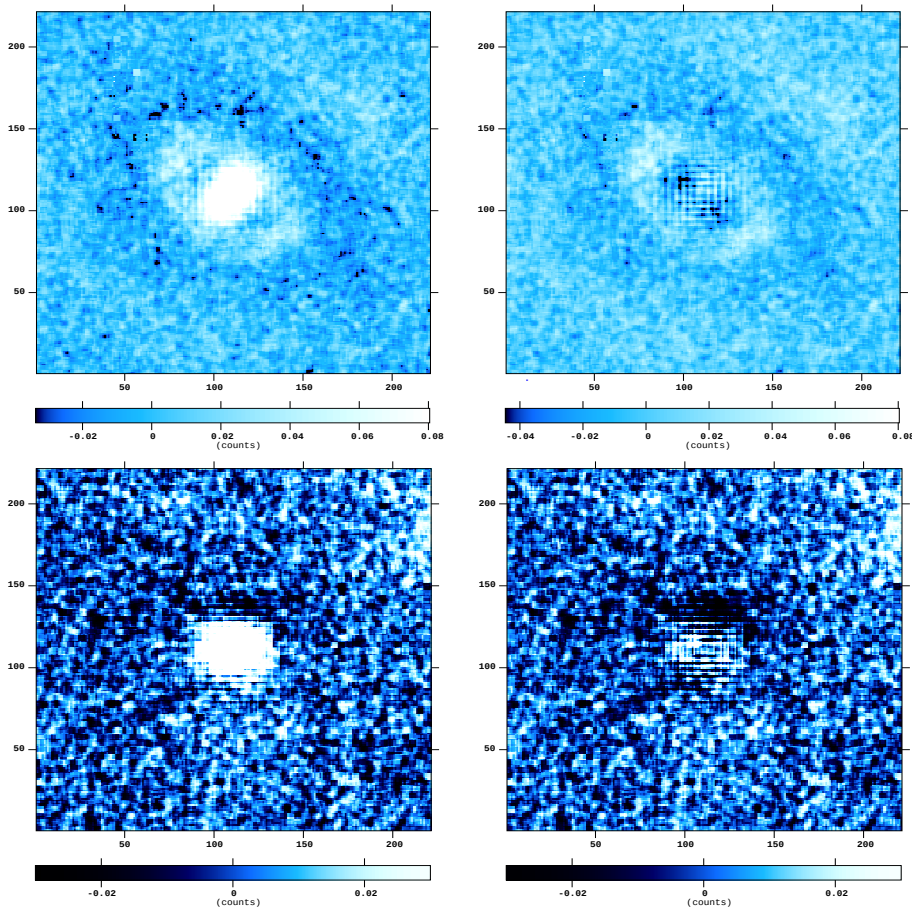

Figure 4. Residual images (galaxy – model) of PKS 03120018 (bottom) and PKS 03120017 (top) obtained applying a model without (on the left) and with (on the right) a central unresolved component.

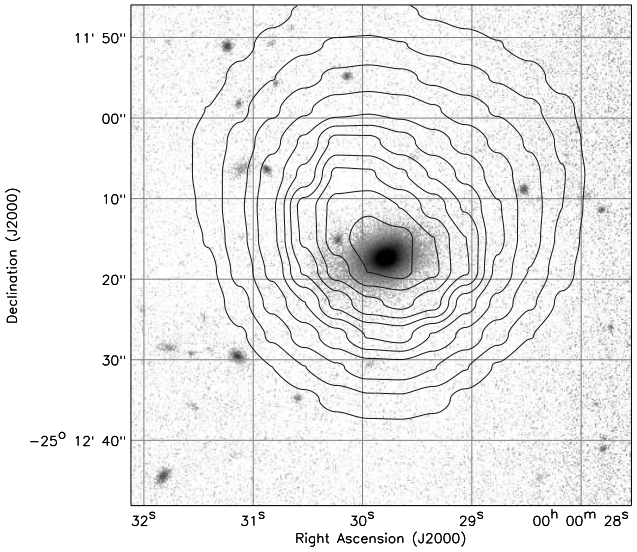

Figure 5. X–ray contours obtained from the 0.5-10 keV adaptively smoothed pn image of source Abell2690013 overlaid on the K_s–band image.

Table 2. Results of the morphological fit performed in the K_s band.

id	m_{host}	r_{eff} (kpc)	$m_{nucleus}$
PKS 03120017	15.25±0.04	5.57±0.80	18.47±0.27
PKS 03120018	15.20±0.01	3.75±0.15	18.07±0.12
Abell 2690013	14.28±0.02	6.76±0.20	–

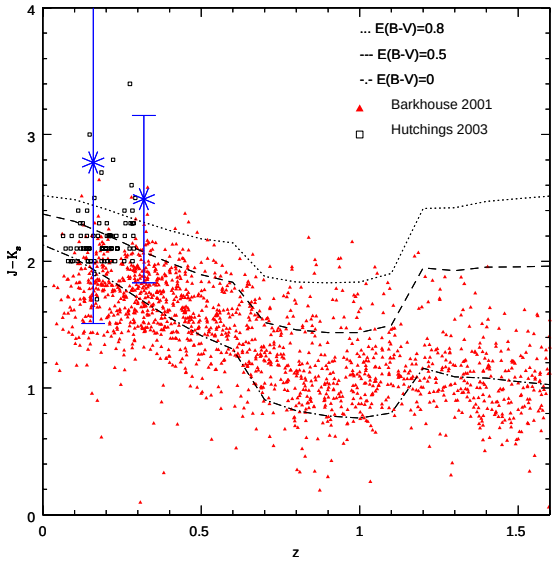

Figure 6. Near–infrared color obtained for the AGNs hosted in PKS 03120018 and 03120017 compared with literature data.

(Cutri et al. 2000), respectively, lending further support to the morphological analysis.

The nuclear J–K_s color of PKS 03120018 and 03120017 is reported in Figure 6 compared with literature data. Red triangles represent the optically selected quasars with near–infrared counterparts in the 2MASS (Barkhouse et al. 2001), the open black squares are the 2MASS selected red quasars from Hutchings et al. (2003) in a redshift range ($0.1 < z < 0.3$) similar to that of our sources. Even if affected by large errors, due to the extremely faint J–band magnitudes, the J–K_s colors are consistent with those of 2MASS red quasars. The tracks plotted in Fig.6 represent the color redshift relations for a quasar template (the composite spectrum from the Large Bright Quasar Survey extended to the near–IR using the mean radio–quiet quasar energy distribution; Francis et al. 2001; Elvis 1994). We have included the effect of internal dust attenuation on the quasar template, using a dust screen model and the SMC extinction law (Pei 1992). The curves represent different extinction values ($E(B-V)$=0, 0.5, 0.8 from bottom to top). At the face value the best fit J–K_s color of the nuclei implies $E(B-V) \simeq 0.8$ which corresponds to $N_H \simeq 5 \times 10^{21}$ cm^{-2} for a standard Galactic dust to gas ratio (Bohlin et al. 1978), in fairly good agreement with the X–ray spectral analysis (see Table 1).

4. SUMMARY

A detailed analysis of deep near–infrared images has allowed us to uncover a weak and red unresolved component in the central region of two bright XBONGs. The red nuclear J-K_s colors suggest the presence of a mildly obscured AGN responsible of the observed X–ray emission. The broad–band properties of two XBONGs are explained by the presence of a mildly obscured nucleus hosted by a bright galaxy. The X–ray luminosity of the third object is most likely due to diffuse emission from hot gas possibly originating in a galaxy group. A more detailed analysis of the XBONG multiwavelength properties, including optical spectral simulations, is currently underway (Civano et al. 2006 in preparation).

ACKNOWLEDGMENTS

Partial support from MIUR Cofin 03–02–23 and INAF/270/2003 grants is acknowledged.

REFERENCES

Barger, A. J., Cowie, L. L., Bautz, M. W., Brandt, W. N., Garmire, G. P., Hornschemeier, A. E., Ivison, R. J., & Owen, F. N. 2001, AJ, 122, 2177

Barkhouse, W. A., & Hall, P. B. 2001, AJ, 121, 2843

Bohlin, R. C., Savage, B. D., & Drake, J. F. 1978, ApJ, 224, 132

Comastri, A., et al. 2002, ApJ, 571, 771

Cutri, R.M., et al., 2000, Explanatory Supplement to the 2MASS Second Incremental Data Release (Pasadena: IPAC)

Elvis, M., et al. 1994, ApJS, 95, 1

Fiore, F., et al. 2003, A&A, 409, 79

Francis, P. J., Hewett, P. C., Foltz, C. B., Chaffee, F. H., Weymann, R. J., & Morris, S. L. 1991, ApJ, 373, 465

Georgantopoulos, I., & Georgakakis, A. 2005, MNRAS, 358, 131

Hornschemeier, A. E., et al. 2001, ApJ, 554, 742

Hutchings, J. B., Maddox, N., Cutri, R. M., & Nelson, B. O. 2003, AJ, 126, 63

Moran, E. C., Filippenko, A. V., & Chornock, R. 2002, ApJ, 579, L71

Pahre, M. A. 1999, ApJS, 124, 127

Pei, Y. C. 1992, ApJ, 395, 130

Peng, C. Y., Ho, L. C., Impey, C. D., & Rix, H. 2002, AJ, 124, 266

Perola, G. C., et al. 2004, A&A, 421, 491

Severgnini, P., et al. 2003, A&A, 406, 483

Yuan, F., & Narayan, R. 2004, ApJ, 612, 724